

## SPECTRAL WAVE CHARACTERIZATION OF THE PACIFIC COAST OF COSTA RICA

GEORGES GOVAERE<sup>1</sup>, HENRY ALFARO<sup>2</sup>

*1 IMARES-UCR, Engineering Research Institute, University of Costa Rica, Costa Rica, georges.govaere@ucr.ac.cr*

*2 IMARES-UCR, Engineering Research Institute, University of Costa Rica, Costa Rica, henry.alfaro@ucr.ac.cr*

### ABSTRACT

The results of the analysis of the wave measurement campaigns on the Pacific coast of Costa Rica are presented. After analyzing more than 14000 spectral shapes from sea states, it has been determined that many of them present 2 or more swell peaks, so it was proposed to perform a wave characterization in which 8 different types of spectra were defined to include all the data collected. Also, verifications were carried out in these sea states to check the reliability of many of the approximations usually used in coastal engineering that assume narrow-band spectra, such as the JONSWAP type.

**KEYWORDS:** Wave measurement, energy spectra, wave analysis, wave characterization.

### 1 INTRODUCTION

The dominant swell reaching the Pacific coast of Costa Rica is produced in the vicinity of New Zealand and Australia. This swell with northeast propagation direction, crosses some 10000 to 12000 km to reach the Pacific coast of Costa Rica and Central America in general, generally taking 10 to 12 days or more to make the transit (Goda,1983), depending on the period of the storm waves, as shown in Figure 1.

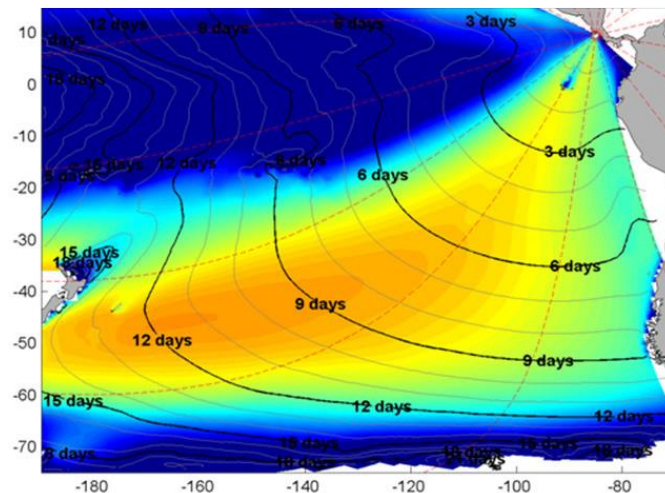


Figure 1. Example of swell travel time to Costa Rica. (Alfaro, 2017).

As these propagation times are so extended, the faster waves of one storm can easily catch up the slower waves of the previous storm, and, when they reach the coast, sea states coming from separate storms can appear at clearly identifiable different frequencies on a single spectrum. On the Pacific coast of Costa Rica, a field campaign has been conducted since 2014 that has allowed us to measure sea states every 3 hours almost continuously, reaching now more than 14000 sea states analyzed. The equipment used in the field campaign are Nortek AWACs, anchored at about 20 m depth in Cabo Blanco, directly exposed to the incident swell from the Southwest.

## 2 RESULTS

A computer program was developed to help visualize and determine which type of spectrum was present in each case. The classification of the 14794 sea state were determined manually.

By analyzing the wave spectra measured, it was determined to group them in 8 different categories, figure 2:

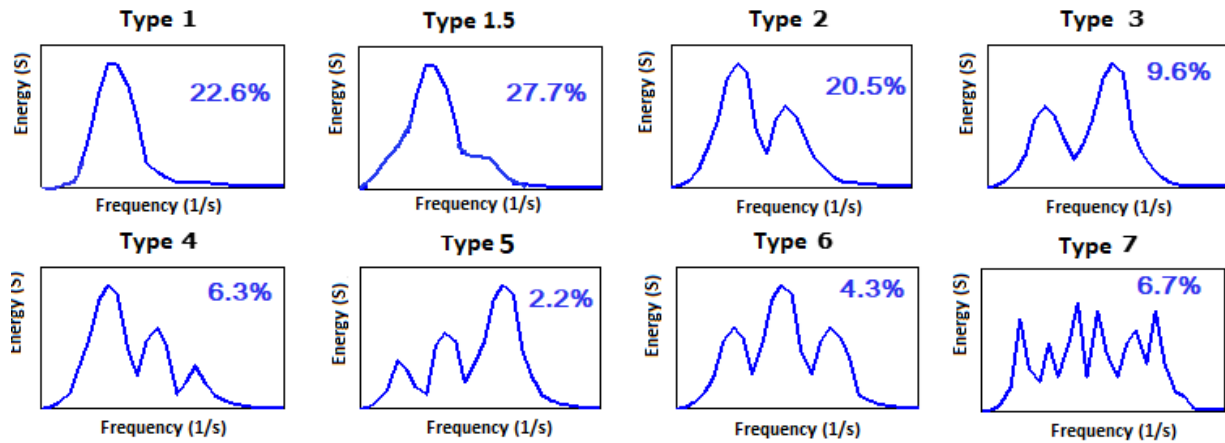
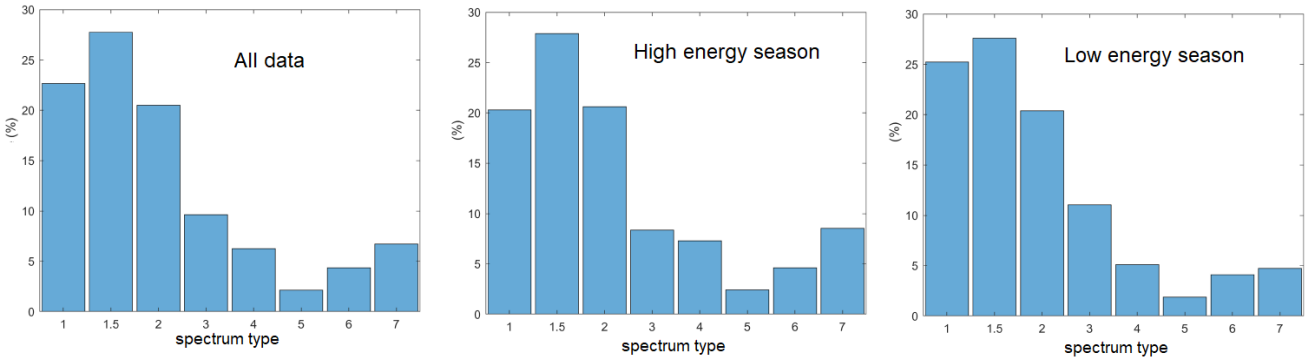


Figure 2. Typical shape of the different types of spectra.

Each of the spectrum types was defined as follows:

- Type 1: Fits a single-peak JONSWAP spectrum. A total of 3350 sea states were recorded for a 22.6% occurrence rate. It was determined from previous analyses that the parameter  $\gamma=7$  is the best fit to the measured data for this type of spectra, instead of the standard  $\gamma=3,3$ .
- Type 1.5: These are single-peak spectra, but the energy dispersion makes them very different from a JONSWAP spectrum. There were 4103 sea states of this type for a 27.7% occurrence rate.
- Type 2: These are spectra in which two energy peaks are clearly observed, where the first peak (low frequency) is higher than the second peak. A total of 3023 sea states of this type were recorded for a 20.5% occurrence rate.
- Type 3: These are spectra in which two energy peaks are clearly observed, where the first peak (low frequency) is lower than the second peak. A total of 1425 sea states of this type were recorded for a 9.6% occurrence rate.
- Type 4: These are spectra in which three energy peaks are clearly observed, where the first peak (low frequency) is the most energetic of the three. A total of 926 sea states of this type were recorded for a 6.3% occurrence rate.
- Type 5: These are spectra in which three energy peaks are clearly observed, where the second peak (intermediate frequency) is the most energetic of the three. A total of 319 sea states of this type were recorded for a 2.2% occurrence rate.
- Type 6: These are spectra in which three energy peaks are clearly observed, where the third peak (highest frequency) is the most energetic of the three. A total of 645 sea states of this type were recorded for a 4.3% occurrence rate.
- Type 7: These are spectra in which more than three energy peaks are observed, or which cannot be classified in any of the previous types. A total of 994 sea states of this type were recorded, for a 6.7% occurrence rate.

It was tested whether there were significant differences according to the season of the year (high or low energy). Although Costa Rica is located in the northern hemisphere, the season of high energy corresponds to the austral winter, so it is taken from May to October. The low energy season would be from November to April.



**Figure 3. Distribution of spectrum types according to season of the year.**

Figure 3 shows that the occurrence of the different types of spectra is approximately the same at all seasons of the year. As energy is presented in a very dispersed way in the spectrum, it was verified that many of the ratios used in engineering such as  $H_s/H_{rms}$ ,  $H_{1/10}/H_{rms}$ ,  $H_{1/100}/H_{rms}$ ,  $H_s/H_{m0}$ ,  $H_{max}/H_s$  and  $T_{m02}/T_z$  are still valid globally and for each one of the identified types of spectra. These relationships assume a narrow band spectrum and a Rayleigh-type wave height distribution, so a different behavior would be expected depending on the energy dispersion in the spectrum for each type. For the temporal analysis, the standard zero up-crossing methodology was used. Figures 4 to 10 show the correlations obtained between the different parameters listed above using all the measured records.

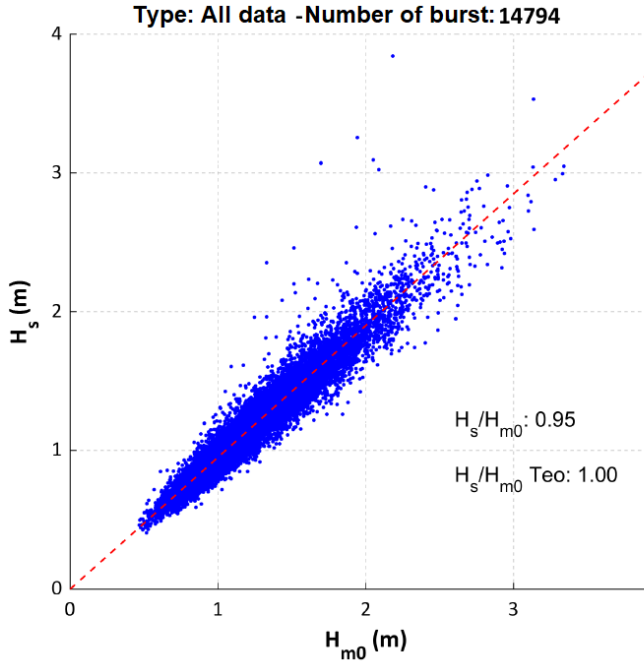


**Figure 4.  $H_s$  vs  $H_{m0}$  for all the data.**

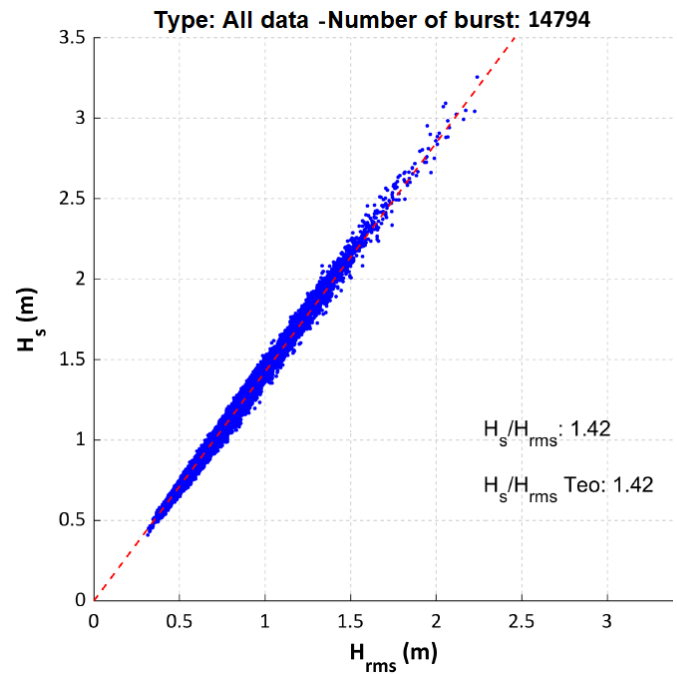


**Figure 5.  $H_s$  vs  $H_{rms}$  for all the data.**

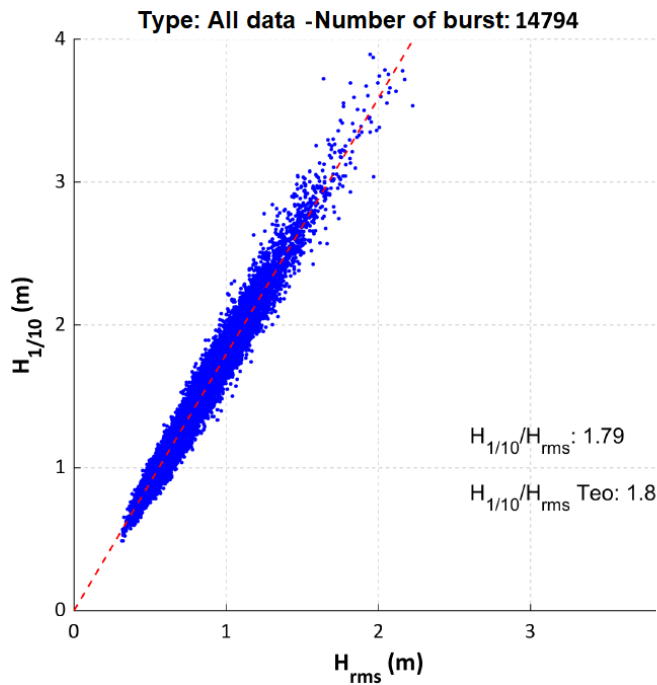


Figure 6.  $H_{1/10}$  vs  $H_{rms}$  for all the data.

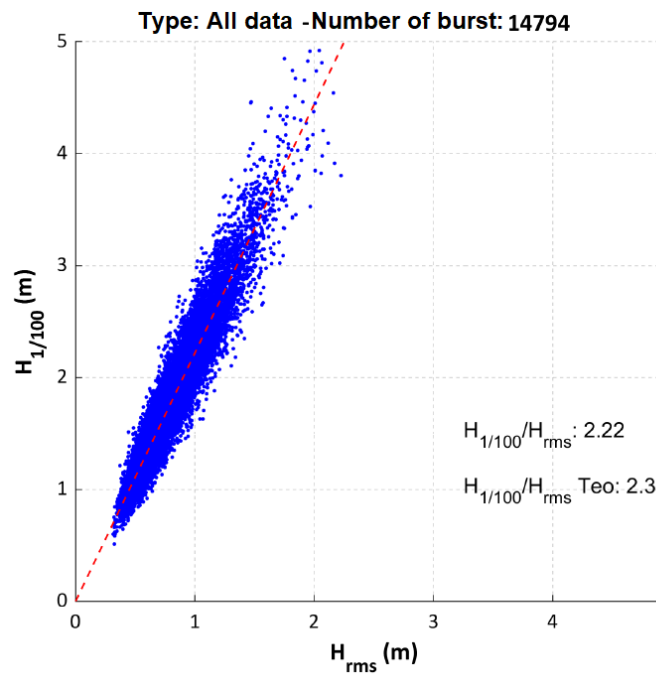


Figure 7.  $H_{1/100}$  vs  $H_{rms}$  for all the data.

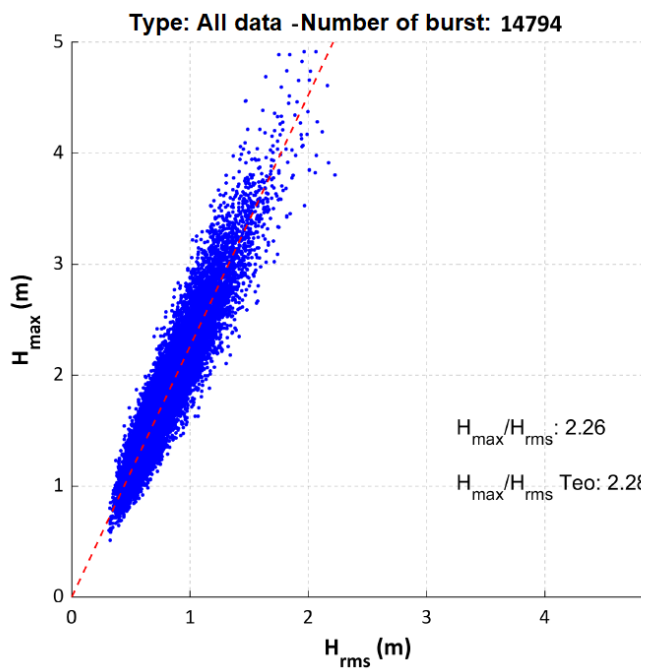


Figure 8.  $H_{max}$  vs  $H_{rms}$  for all the data.

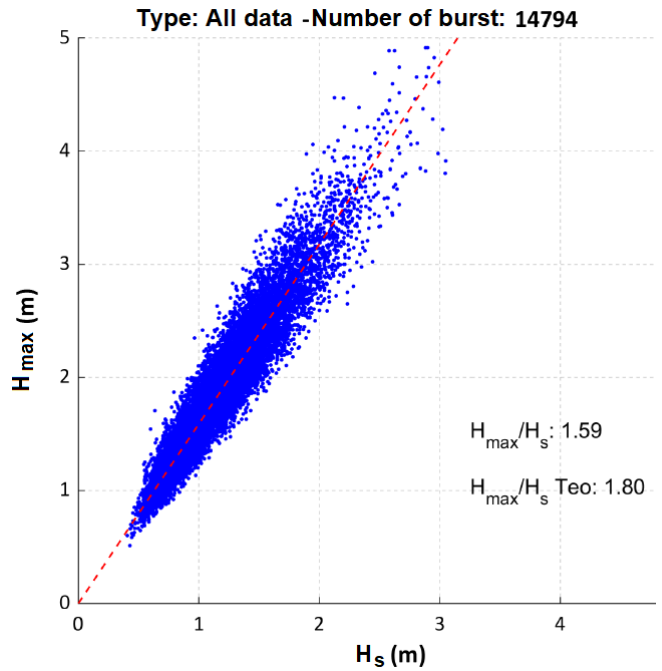


Figure 9.  $H_{max}$  vs  $H_s$  for all the data.

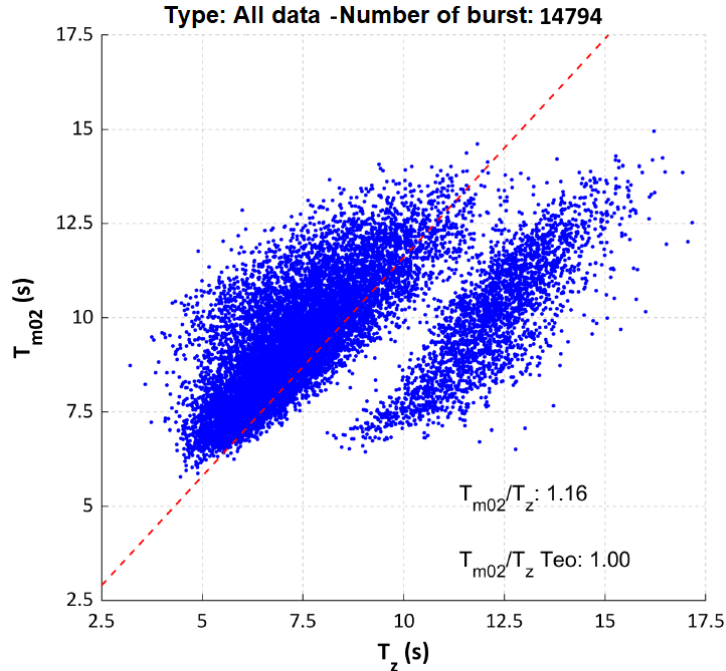


Figure 10.  $T_{m02}$  vs  $T_z$  for all the data.

The behavior of  $T_{m02}$  versus  $T_z$ , figure 10, is quite interesting, showing a large scatter of data and what clearly appear to be two "families" of data. This behavior was present in all the spectrum types. The same procedure is applied for all types of spectra from 1 to 7, finding a similar data dispersion. As an example, the relationship between  $H_{1/100}$  and  $H_{rms}$  is presented for spectrum types 1, 1.5, 2 and 3 in figures 11, 12, 13 and 14.

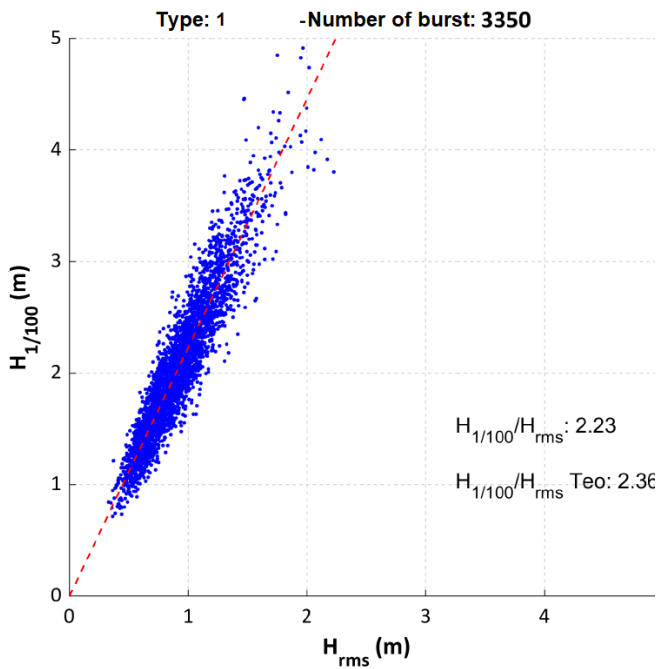


Figure 11.  $H_{1/100}$  vs  $H_{rms}$  for the type 1 spectra.

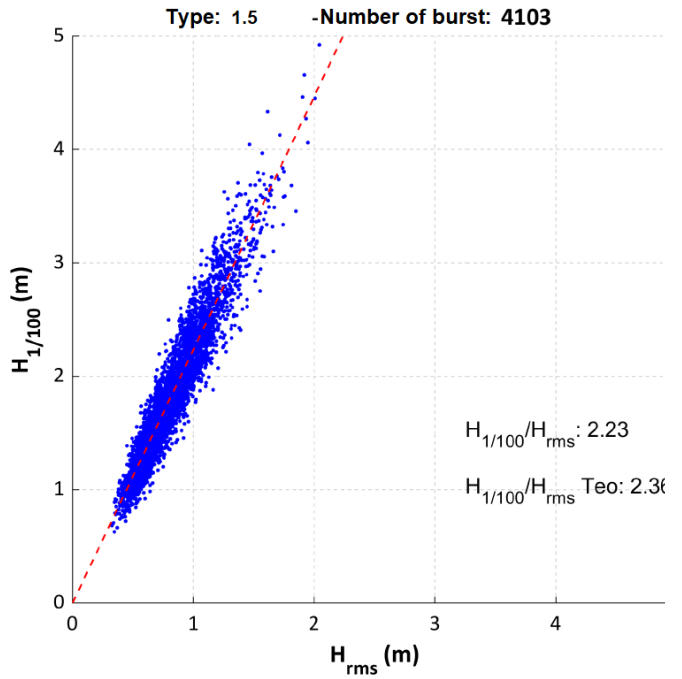


Figure 12.  $H_{1/100}$  vs  $H_{rms}$  for the type 1.5 spectra.

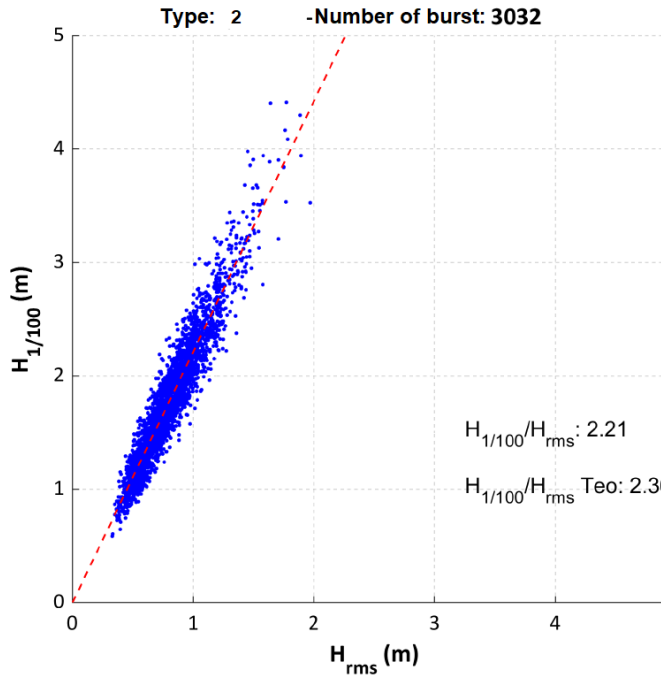


Figure 13.  $H_{1/100}$  vs  $H_{rms}$  for the type 2 spectra.

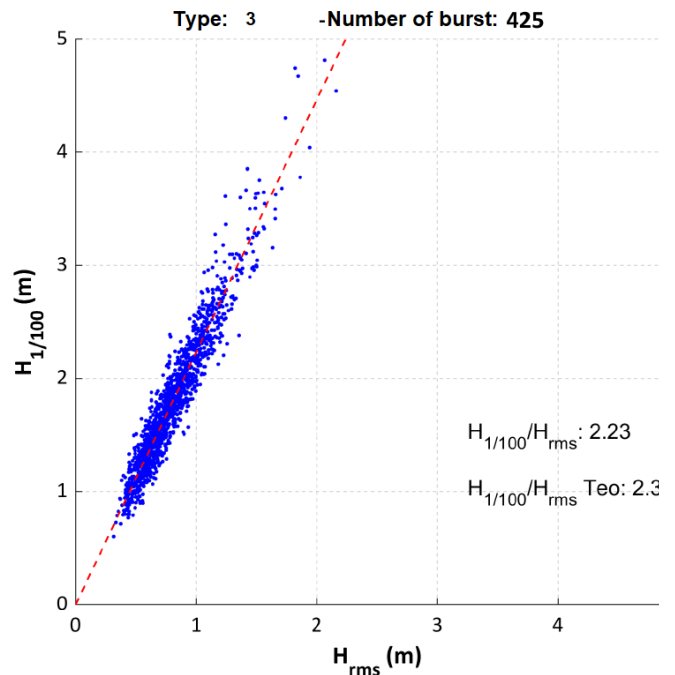


Figure 14.  $H_{1/100}$  vs  $H_{rms}$  for the type 3 spectra.

The relationships found between all parameters and for all spectrum types are summarized in Table 1.

**Table 1. Summary of all engineering relationships for all data, for each spectrum type and for theory**

| Type     | $H_s/H_{rms}$ | $H_{1/10}/H_{rms}$ | $H_{1/100}/H_{rms}$ | $H_{max}/H_{rms}$ | $H_s/H_{m0}$ | $H_{max}/H_s$ | $H_{rms}/\sqrt{m_0}$ | $T_{m02}/T_z$ |
|----------|---------------|--------------------|---------------------|-------------------|--------------|---------------|----------------------|---------------|
| All data | 1.424         | 1.794              | 2.22                | 2.262             | 0.95         | 1.589         | 2.668                | 1.16          |
| 1        | 1.436         | 1.818              | 2.23                | 2.256             | 0.937        | 1.571         | 2.609                | 1.167         |
| 1.5      | 1.427         | 1.803              | 2.234               | 2.274             | 0.95         | 1.593         | 2.662                | 1.166         |
| 2        | 1.418         | 1.782              | 2.211               | 2.259             | 0.953        | 1.593         | 2.688                | 1.149         |
| 3        | 1.424         | 1.793              | 2.233               | 2.278             | 0.954        | 1.601         | 2.681                | 1.16          |
| 4        | 1.412         | 1.765              | 2.187               | 2.244             | 0.962        | 1.589         | 2.725                | 1.149         |
| 5        | 1.406         | 1.754              | 2.182               | 2.237             | 0.963        | 1.591         | 2.74                 | 1.129         |
| 6        | 1.411         | 1.769              | 2.209               | 2.269             | 0.955        | 1.608         | 2.707                | 1.149         |
| 7        | 1.407         | 1.755              | 2.181               | 2.245             | 0.969        | 1.596         | 2.756                | 1.166         |
| Theory   | 1.416         | 1.8                | 2.359               | 2.28              | 1            | 1.8           | 2.8284               | 1             |

Although some values are slightly different from those presented in the literature, in most cases a similar behavior was maintained regardless of the type of spectrum. Surprisingly, the values that deviate the most from the theoretical values are those of the type 1 spectra, which conform to the "JONSWAP" type, contrary to what was initially expected. All the data presented in Table 1 were repeated for the division made between the high energy and low energy seasons. The results presented in table 2 and 3 show approximately the same behavior.

**Table 2. Summary of all engineering relationships for the low energy season data, for each spectrum type and for theory**

| Type   | Hs/Hrms | H <sub>1/10</sub> /Hrms | H <sub>1/100</sub> /Hrms | Hmax/Hrms | Hs/Hm0 | Hmax/Hs | Hrms/√m0 | Tm02/Tz |
|--------|---------|-------------------------|--------------------------|-----------|--------|---------|----------|---------|
| Low En | 1.42    | 1.79                    | 2.211                    | 2.245     | 0.939  | 1.581   | 2.646    | 1.106   |
| 1      | 1.431   | 1.806                   | 2.206                    | 2.228     | 0.936  | 1.557   | 2.616    | 1.126   |
| 1.5    | 1.423   | 1.8                     | 2.231                    | 2.266     | 0.942  | 1.593   | 2.649    | 1.118   |
| 2      | 1.413   | 1.776                   | 2.197                    | 2.234     | 0.939  | 1.581   | 2.659    | 1.089   |
| 3      | 1.42    | 1.793                   | 2.233                    | 2.272     | 0.941  | 1.6     | 2.65     | 1.113   |
| 4      | 1.407   | 1.764                   | 2.197                    | 2.241     | 0.941  | 1.593   | 2.675    | 1.074   |
| 5      | 1.396   | 1.736                   | 2.174                    | 2.224     | 0.932  | 1.594   | 2.671    | 1.035   |
| 6      | 1.406   | 1.765                   | 2.2                      | 2.248     | 0.934  | 1.599   | 2.657    | 1.074   |
| 7      | 1.399   | 1.744                   | 2.166                    | 2.214     | 0.948  | 1.582   | 2.71     | 1.06    |
| Theory | 1.416   | 1.8                     | 2.359                    | 2.28      | 1      | 1.8     | 2.8284   | 1       |

**Table 3. Summary of all engineering relationships for the high energy season data, for each spectrum type and for theory**

| Type    | Hs/Hrms | H <sub>1/10</sub> /Hrms | H <sub>1/100</sub> /Hrms | Hmax/Hrms | Hs/Hm0 | Hmax/Hs | Hrms/√m0 | Tm02/Tz |
|---------|---------|-------------------------|--------------------------|-----------|--------|---------|----------|---------|
| High En | 1.427   | 1.797                   | 2.226                    | 2.274     | 0.957  | 1.594   | 2.683    | 1.219   |
| 1       | 1.441   | 1.828                   | 2.251                    | 2.279     | 0.938  | 1.582   | 2.603    | 1.221   |
| 1.5     | 1.43    | 1.805                   | 2.236                    | 2.28      | 0.955  | 1.594   | 2.671    | 1.217   |
| 2       | 1.421   | 1.785                   | 2.22                     | 2.276     | 0.962  | 1.601   | 2.707    | 1.215   |
| 3       | 1.427   | 1.794                   | 2.233                    | 2.284     | 0.966  | 1.601   | 2.707    | 1.231   |
| 4       | 1.414   | 1.766                   | 2.183                    | 2.245     | 0.972  | 1.587   | 2.748    | 1.205   |
| 5       | 1.412   | 1.764                   | 2.186                    | 2.244     | 0.98   | 1.589   | 2.778    | 1.212   |
| 6       | 1.414   | 1.771                   | 2.215                    | 2.281     | 0.967  | 1.613   | 2.736    | 1.224   |
| 7       | 1.409   | 1.759                   | 2.186                    | 2.256     | 0.977  | 1.601   | 2.774    | 1.231   |
| Theory  | 1.416   | 1.8                     | 2.359                    | 2.28      | 1      | 1.8     | 2.8284   | 1       |

### 3 CONCLUSIONS

After starting to measure waves in the Pacific of Costa Rica, it was detected that the wave periods are very high and that many times there were spectra of 2 peaks or more, so it was decided to carry out an extensive field campaign in order to characterize the waves in this area of the Pacific. From the data analysis it was concluded that an 8-segment classification can represent the totality of the measured wave spectra. It should be noted that the typical design conditions, usually a JONSWAP type spectrum, is presented in less than 23% of the time and 28% of the time a spectrum of a single peak is presented, but it cannot be approximated to a JONSWAP because it has a large amount of energy dispersed in many frequencies. Spectra of 2, 3 or more peaks are present 50% of the time. Although the spectra presented on the Pacific coast of Costa Rica have a large energy dispersion, the commonly used engineering approximations are still valid, although in some cases with slightly different values than those reported in the literature.

### REFERENCES

- Alfaro\_Chavarría, H, 2017. *Estudio de la dinámica del oleaje en el litoral pacífico de Costa Rica, metodologías de regionalización y avances en servicios relativos al clima marítimo*. PhD Thesis, Universidad de Cantabria, Spain.
- Goda, Y, 1983. *Analysis of wave grouping and spectra of long-travelled swell*. Rep Port and Harbour Res. Inst. vol 22, no.1, pp3-41